Analysis of Planar Strip Array Antenna for MRI

Ray F. Lee[1], Charles R. Westgate[2]

[1]GE, Corporate Research & Development, Niskayuna, NY, 12309; [2]Johns Hopkins University, Electrical and Computer Engineering Department, Baltimore, MD 21218

***Abstract* — With a large number of RF detectors, a sequential MRI data acquisition could become a parallel process, thus reducing scan time significantly. PSA provides a means for such massive parallel detection. The theoretical analyses of the reactive field, coupling, and Q-factors of PSA are presented, and they were validated by the experimental measurements of the *in vivo* MRI with PSA.**

I. INTRODUCTION

The "MRI phased array" [1] has been widely used in clinical scanners for increasing signal-to-noise (SNR) and field of view (FOV). Unlike far-field phased array antennas, the MRI phased array works in the reactive field region and requires isolation between the element detectors. Due to the element loop structure and the difficulty in isolating the coils, the number of coils in a conventional MRI phased array is very limited, usually between four to eight.

Recently the parallel spatial encoding techniques in MRI [2] has been shown to be a practical method for significantly reducing the minimum scan time by replacing phase-encoding steps with the encoding inherent in the sensitivity profiles of a set of phased array coils. To completely replace the phase encoding steps while sustaining the image resolution, the number of the element coils of the order of 10^2 is required The conventional MRI phased array cannot meet this challenge.

Here we introduce a new type of array detector, the planar strip array (PSA)[3]. Its structure is an array of parallel commensurate length microstrips with a layer of overlay on top. Both the substrate and overlay have the same high relative permittivity (ε_r) which reduces the EM field wavelength by a factor of $\sqrt{\varepsilon_r}$ to make a quarter wavelength ($\lambda/4$) resonator at the MRI frequency (63.9MHz at 1.5T) with a reasonable length for a MRI detector.

The PSA has two advantages compared to the conventional MRI phased array. First, the length of the strips in the PSA can be adjusted such that the coupling between the strips vanishes: the strips are isolated regardless of spacing. Thus it can accommodate a large number of detectors for simultaneous acquiring MRI signals without interference between element detectors. Second, with appropriate termination, a standing wave occurs on the isolated strips providing a high SNR

II. A RIGID ANALYSIS OF PSA

The structure of the PSA is shown in Fig. 1. Because our GE MRI scanner is limited to only 4 receiver channels, 4 copper strips are laid in parallel between 2 sheets of glass. The dielectric constant of glass is $\varepsilon_r = 6.4$. The $\lambda/4$ of the proton MR frequency at 1.5T (63.87MHz) in air is 117cm, but in glass it is only 46cm. The strips are surrounded by a grounded guard ring. The strip length l can be either $\lambda/4$ or $\lambda/2$. The strip width w, spacing s, and thickness of the dielectric h, determine the characteristic impedance of the strip Z_0. At both ends of the strip, BNC panel connectors are installed to provide feeding points and terminations.

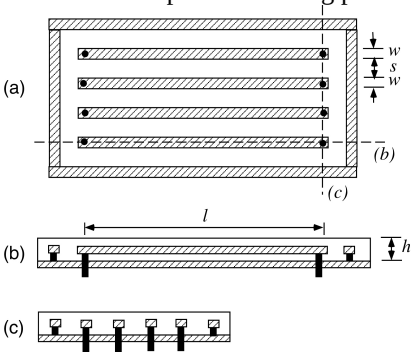

Fig. 1 PSA's structure: (a) is plane view, (b) is side view, and (c) is end elevation. The shaded strips are conductors.

When the strip length is an integer times $\lambda/4$ and its termination is either open or a short, the PSA is called a standing wave PSA (SW-PSA). When the strip length is an integer times $\lambda/2$ and its termination is a matched load, the PSA is called a travelling wave PSA (TW-PSA).

A. The reactive near-field of the strip

Since the region that PSA detects is less than one wavelength, the EM field in this region is mainly reactive near-field. The magnetic field sensitivity of one PSA strip can be derived from the Biot-Savart Law, image method, and the reciprocity principle with a given current distribution $f(\xi)$ on strips. Assume that the feeding point is at $\xi=0$ and the termination is at $\xi=l$ in the Fig. 2. For TW-PSA, $f(\xi)=1$; for SW-PSA with short termination, $f(\xi)=2\sin\beta\xi$; and for SW-PSA with open termination,

$f(\xi)=2\cos\beta\xi$. Here $\beta=2\pi/\lambda$. The magnetic field sensitivity is $B(x,z)=$

$$\frac{\mu I_0}{4\pi}\int_0^l\left(\frac{z}{\left((\xi-x)^2+z^2\right)^{3/2}}-\frac{z+h}{\left((\xi-x)^2+(z+h)^2\right)^{3/2}}\right)f(\xi)d\xi\,. \quad (1)$$

Here I_0 is the travelling wave current on the strip.

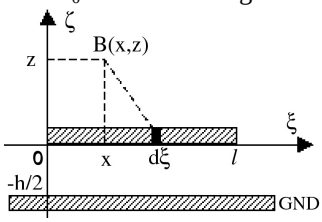

Fig. 2 Descriptions of the parameters used in Eq. (1).

B. The isolation between the strips

The coupling between any two strips can be analyzed with even-odd mode theory. At the feeding point, Γ_e and Γ_o are the even and odd mode input reflection of strip, and Γ_G is the source reflection. Thus the coupling coefficient is

$$k=\frac{1}{2}\frac{\Gamma_e-\Gamma_o}{1-\Gamma_G(\Gamma_e+\Gamma_o)/2}\,. \quad (2)$$

The coupling between two SW-PSA strips can be derived from Eq. (2) and ABCD matrix of the transmission line. Assume that the attenuation is trivial, $\alpha\approx 0$. When the strip is terminated with a short, the coupling, *k*, is:

$$k=\frac{j(\bar{Z}_{0e}-\bar{Z}_{0o})\sin 2\beta l}{2(\cos^2\beta l-\bar{Z}_{0o}\bar{Z}_{0e}\sin^2\beta l)+j(\bar{Z}_{0o}+\bar{Z}_{0e})\sin 2\beta l+g},$$

where $g=2\Gamma_G(\bar{Z}_{0o}\bar{Z}_{0e}\sin^2\beta l+\cos^2\beta l)$. (3)

Here $\bar{Z}_{0e}$ and $\bar{Z}_{0o}$ are the normalized even and odd mode input impedance of the strips. When $l=\lambda/4$, $\beta l=\pi/2$, and $\sin 2\beta l=0$ (provided that $\Gamma_G\neq 1$) $k=0$, and there is no coupling between any two strips in the SW-PSA. But if $\Gamma_G=1$, the $\sin 2\beta l$ term cancels, the coupling becomes maximum.

When any two SW-PSA strips are terminated with open circuit, the *k* becomes:

$$k=\frac{j(\frac{1}{\bar{Z}_{0o}}-\frac{1}{\bar{Z}_{0e}})\sin 2\beta l}{2(\cos^2\beta l-\frac{\sin^2\beta l}{\bar{Z}_{0o}\bar{Z}_{0e}})+j(\frac{1}{\bar{Z}_{0o}}+\frac{1}{\bar{Z}_{0e}})\sin 2\beta l-g},$$

where $g=2\Gamma_G\left(\frac{\sin^2\beta l}{\bar{Z}_{0o}\bar{Z}_{0e}}+\cos^2\beta l\right)$. (4)

Equation (4) again indicates that when $l=\lambda/4$, and $\sin 2\beta l=0$, there is no coupling between strips provided that $\Gamma_G\neq -1$. Otherwise the coupling is maximum.

For the TW-PSA, the strip terminations are the matched loads, the coupling coefficient between two strips is

$$k=\frac{j(\bar{Z}_{0e}-\bar{Z}_{0o})\sin\beta l}{2\cos\beta l+j(\bar{Z}_{0o}+\bar{Z}_{0e})\sin\beta l}\,. \quad (5)$$

At $l=\lambda/2$, $\beta l=\pi$, and $\sin\beta l=0$, and no coupling occurs between the strips.

Equations (3-5) indicate that there are two ways to isolate the strips. One is to select the proper strip length to make $\sin 2\beta l$ (SW-PSA) or $\sin\beta l$ (TW-PSA) equal to zero, and narrow-band decoupling is achieved. The simulations of the narrow-band decoupling are shown in Fig. 3.

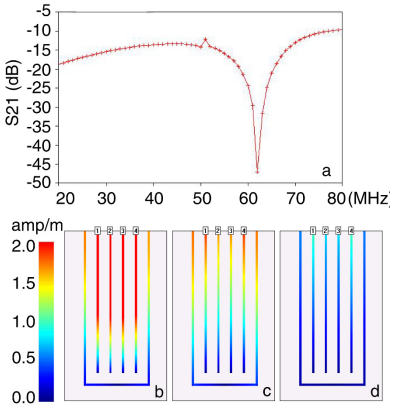

Fig. 3 The simulations of an open SW-PSA. (a) is S21 of a pair of strips. (b), (c), and (d) are the current distributions if $l=\lambda/4$, $3\lambda/16$, and $\lambda/8$.

Another way for isolation is to make $\bar{Z}_{0e}=\bar{Z}_{0o}$, since Z_{0e} and Z_{0o} only depend on the transverse dimensions (*s*, *w*, and *h*) [3,4], and broadband decoupling is achieved. The condition of broadband decoupling is

$$1+\tanh(\frac{\pi}{2}\frac{s}{h})=(1+\coth(\frac{\pi}{2}\frac{s}{h}))^2\Big/2\,. \quad (6)$$

The graphic solution of the Eq. (6) is in Fig. 4.

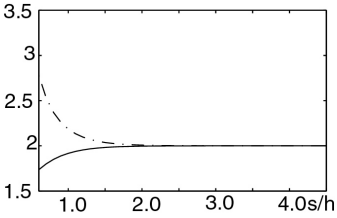

Fig. 4 The solid line is the left side of Eq. (6), and the dash line is the right side of Eq. (6).

When the ratio $s/h>2.5$, there is a broadband isolation between the strips.

C. The Q-factor of the strip [5]

The unloaded Q: If the attenuation constant α is very small and $(\alpha l)^2<<1$, the unloaded Q-factor of the transmission line resonator is

$$Q_U\approx\beta/2\alpha\,. \quad (7)$$

Here α can be estimated from the conductor loss and dielectric loss.

The external Q: When the strips are connected with the external circuit, Q_E is the ratio of the energy stored in the

0-7803-6540-2/01/$10.00 (C) 2001 IEEE

strip to the energy dissipated in the resistive outside of the strips. The resistive load, R_E, can include the equivalent resistance of the imaging object load, the resistance of the preamplifier, and the cable loss, etc. In general, direct-coupling results in a low Q_E. For example, a λ/4 strip terminated with either a short or an open circuit has a Q_E that is either

$$Q_E = \frac{R_E}{2Z_0}\frac{\pi}{2}, \text{ or } Q_E = \frac{Z_0}{2R_E}\frac{\pi}{2}. \quad (8)$$

Thus, the Q_E of the directly-coupled strip depends only on the Z_0 and R_E, and its values are close to unity when Z_0 and R_E are comparable.

To control and increase Q_E, the reactive-coupling between the strip and preamplifier can be used. Here two special cases, an open and a short λ/4 strip, are analyzed to demonstrate the enhancement of Q_E using reactive coupling. In the first case when the strip is terminated with a short, a series capacitor C is needed for coupling the signal out of the strip. Its input reactance is $X = -1/\omega C + Z_0 \tan\beta l$, $\beta = \omega/v$, and v is the phase velocity. The external Q-factor is:

$$Q_E = \frac{Z_0}{2R_E}\left(\frac{1}{\omega_r C Z_0} + \beta l(1+\tan^2\beta l)\right). \quad (9)$$

At the resonance frequency ω_r, the reactance X=0, and therefore

$$\frac{1}{\omega_r C}\frac{1}{Z_0} = \tan\beta l = \overline{X}_c, \quad (10)$$

where $\overline{X}_c$ is the magnitude of the normalized reactance of the capacitor. Substituting Eq. (10) into Eq. (9) then yields:

$$Q_E = \frac{Z_0}{2R_E}\left(\overline{X}_c + \beta l(1+\overline{X}_c^2)\right). \quad (11)$$

In the case when the strip is open circuit, a shunt inductor L is needed for coupling the signal out of the strip. Its input susceptance is $B = -1/\omega L + Y_0 \tan\beta l$. The external Q_E is

$$Q_E = \frac{Y_0}{2G_E}\left(\frac{1}{\omega_r L Y_0} + \beta l(1+\tan^2\beta l)\right), \quad (12)$$

where $G_E=1/R_E$ and $Y_0=1/Z_0$. At the resonant frequency, ω_r, the susceptance B=0. Therefore

$$\frac{1}{\omega_r L}\frac{1}{Y_0} = \tan\beta l = \overline{B}_L, \quad (13)$$

where $\overline{B}_L$ is the magnitude of the normalized susceptance of the inductor. Substituting Eq. (13) into (12) yields

$$Q_E = \frac{R_E}{2Z_0}\left(\overline{B}_L + \beta l(1+\overline{B}_L^2)\right) \quad (14)$$

The Loaded Q**:** Q_L is the ratio of the energy stored in the strip to the total energy losses in the strips, external circuits, the subject being imaged, and the cables. Q_L can be calculated by $1/Q_L=1/Q_U+1/Q_E$.

In the case of the reactively coupled λ/4 strip terminated with a short circuit, based on Eqs. (7,11), the Q_L is:

$$Q_L = \frac{Z_0(\overline{X}_c + \beta l(1+\overline{X}_c^2))}{Z_0(\overline{X}_c + \beta l(1+\overline{X}_c^2))(2\alpha/\beta) + 2R_E}. \quad (15)$$

If the λ/4 strip is terminated with an open circuit, then its Q_L, from Eqs. (7,14), is:

$$Q_L = \frac{R_E(\overline{B}_L + \beta l(1+\overline{B}_L^2))}{R_E(\overline{B}_L + \beta l(1+\overline{B}_L^2))(2\alpha/\beta) + 2Z_0} \quad (16)$$

The behaviors of Q_L calculated from Eq. (15) and (16) are plotted in Fig. 5.

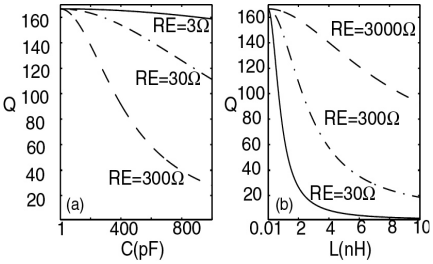

Fig. 5 The effects of the reactive coupling elements on loaded Q

III. EXPERIMENTS

A λ/4 SW-PSA prototype was built. Its dielectric medium is glass (er=6.4). Its length is *l*=46cm. The strip width *w* = 0.635cm, spacing *s* = 3.175cm and dielectric thickness, *h* = 1.27cm. All of the antenna strips are parallel to the direction of the static magnetic field of the magnet bore. At the feeding point each strip is connected to a RF-screened box containing a PIN diode T/R switch and a DC blocking and coupling capacitor.

The performance of the PSA was measured with S-parameters on a Hewlett-Packard network analyzer (HP 8722D and HP 4195A; Hewlett Packard, Palo Alto, CA) and GE *signa* and *LX* 1.5 T MRI scanners (GE Medical Systems, Milwaukee, WI). The S21 measurements confirmed the decoupling predicted by Equations (3) and (4). MRI was performed to show that the PSA is a viable near-field array detector for *in vivo* MRI.

A. Isolation measurements

Equations (3) and (4) indicate that the SW-PSA have both narrow-band and broadband decoupling. The narrow-band decoupling occurs when the strips lengths are nearly an integer number of λ/4, and the broadband decoupling occurs when the ratio of *s*/*h*>2.5. Both types of isolation can be measured by the *S21* parameter on the network analyzer. The *S*-parameter measurement reveals that our prototype SW-PSA with short termination has approximately –30dB narrow-band and –30dB broadband

isolation when it is loaded. As shown in Fig. 6, the total isolation at the resonance frequency is about –60dB.

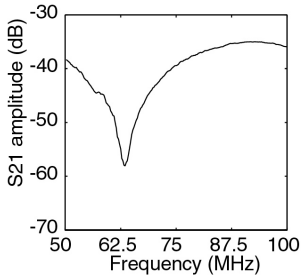

Fig. 6 The S21 measured at feeding points of two adjacent strips. It shows both narrow-band and broadband decouplings.

B. Sequential and parallel encoded MRI

The PSA can be used in MRI with conventional phase-encoding steps. It has the potential of providing a large number of strips to boost SNR and FOV. An *in vivo* MRI of the human knee was acquired with gradient echo pulse sequences using the 4-element PSA and is shown in Fig. 7.

Fig. 7 A gradient echo human leg image acquired with PSA and sequential spatial encoding (NEX=2, TR=500ms, TE=11ms).

PSA can also be used in parallel spatial encoded MRI. Using the PSA as a RF detector array and ASP [3] as a reconstruction method, a sensitivity-encoded MRI experiment was performed on a phantom with a decimation factor of two (scan time reduce half). The results showing the individual decimated images from the four channels of the PSA, and an image reconstructed with ASP, are shown in Fig. 8 a, b, c, d, and e.

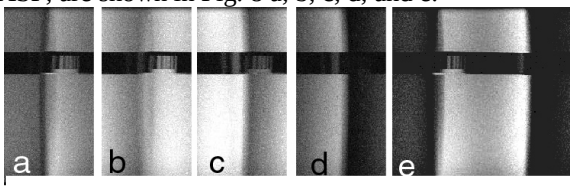

Fig. 8 A phantom image acquired with PSA and partial parallel spatial encoding. (a), (b), (c), and (d) are the decimated images from four channel PSA. (e) is the image reconstructed from (a), (b), (c), and (d) by ASP method.

IV. Discussion

A. SNR of the PSA

For a given receive bandwidth and temperature [6], the SNR is proportional to

$$SNR \sim B/\sqrt{R_E} \ . \qquad (17)$$

Here B can be calculated from Eq. (1), and the noise resistance R_E can be estimated from Eq. (15) or (16) based on the loaded Q_L measurement.

B. Design of a λ/4 shorted SW-PSA

If l is exactly λ/4, C=0 is required to tune the strip, see Eq. (10). Equation (15) indicates that if C=0, increasing load (R_E) does not affect the loaded Q_L at all, so the PSA can barely detect an MR signal. Also C=0 makes Γ_G=1, According to Eq. (3), this leads to the maximum narrow-band coupling, because the $\sin 2\beta l$ terms in Eq (3) are cancelled. To avoid these situations, the strip length l should be slightly less than λ/4. To keep the strip resonant, a series capacitor C, determined by Eq. (10), is needed.

The transverse dimensions (h, s, and w) also have direct impacts on both SNR and decoupling, since the $\overline{Z}_0^e$ and $\overline{Z}_0^o$ depend on h, s, and w. The difference $Z_0^e - Z_0^o$ determines the broadband decoupling factor in Eq. (3). The larger the s/h ratio, the less broadband coupling. Although increasing h causes more broadband coupling, the larger h can improve the sensitivity B, as indicated in Eq. (1).

V. Conclusion

The massive parallel RF detection in MRI demands a new type of array detector. It requires that each element detector should be simple and any pair of elements should be isolated. The PSA is designed for such a purpose, and it is shown that it is a valid approach.

References

[1] P. B. Roemer, et al, "The NMR phased array," *Magn. Reson. Med.*, vol. 16, pp. 192-225, 1990.

[2] R. F. Lee, et al, "An analytical SMASH procedure (ASP) for sensitivity-encoded MRI," *Magn. Reson. Med.*, vol. 43, pp. 716-725, 2000.

[3] R. F. Lee, et al, "The planar strip array (PSA) for MRI," *Magn. Reson. Med.*, accepted.

[4] S. B. Cohn, "Shielded coupled-strip transmission line," *IRE Trans. Microwave Theory and Tech.*, vol. MTT-3, pp. 29-38, Oct. 1955.

[5] P. A. Rizzi, *Microwave Engineering passive circuits*, New Jersey: Prentice Hall, 1988.

[6] J. Wang, et al, "Calculation of the signal-to-noise ratio for simple surface coils and arrays of coils," *IEEE Trans. Biomed. Eng.*, vol. 42, pp. 908-917, 1995.